

CORRECTING HOTWIRE MISALIGNMENT ERRORS FOR WALL-BOUNDED TURBULENCE MEASUREMENTS

Rahul Deshpande¹, Jason P. Monty¹, Ivan Marusic¹

¹Department of Mechanical Engineering,
 The University of Melbourne, Victoria 3010, Australia
 email: raadeshpande@gmail.com

ABSTRACT

In case of wall-bounded flows, the lateral velocity fluctuations measured via hotwire anemometry (e.g. X-probes) are extremely sensitive to calibration of the multi-wire probe. In the present study, we propose a scheme to correct these velocity statistics which are rendered inaccurate due to misalignments during probe calibration. The method is based on the well accepted argument that the viscous-scaled small-scale turbulence energy is invariant with Reynolds number. The scheme is shown to work well for data acquired using X-probes of varying measuring volume and across a decade of Re_τ .

INTRODUCTION

Multi-wire probe measurements are prone to various errors. Apart from the errors due to spatial resolution (Philip *et al.*, 2013; Baidya *et al.*, 2019b), uncertainties in the calibration procedure of probes also bring in additional errors and these have been investigated to a limited extent in the literature (Yavuzkurt, 1984; Jørgensen, 1996). For a multi-wire probe, a two-dimensional (2-D) calibration is conducted to map the relationship between the three velocity components and the corresponding voltages from each sensor. Jørgensen (1996) found that the lateral velocity fluctuations are more sensitive to the uncertainties in the 2-D calibration than the streamwise velocity fluctuations.

Recently, Baidya *et al.* (2019a) have utilized channel DNS flow fields to investigate the sensitivity of the turbulent stresses to the misalignment of a 2-D calibration. A 2-D calibration is said to be misaligned when the coordinate system of the jet does not align with the coordinate system of the wind-tunnel. Figure 1 explains this for the case of a uw X-probe with x , y and z denoting the streamwise, spanwise and wall-normal directions respectively, with u , v and w denoting the velocities corresponding to these directions (this convention is followed throughout the manuscript). Baidya *et al.* (2019a) showed that all the turbulence stresses are adversely affected by the misalignment, especially the Reynolds shear stress (\overline{uw}). Further, they proposed that the angular misalignment for 2-D calibration can be accounted for by rotating the jet reference plane to match a reference ‘zero-angle’ calibration performed in the wind tunnel. This practise, however, was found to be effective for

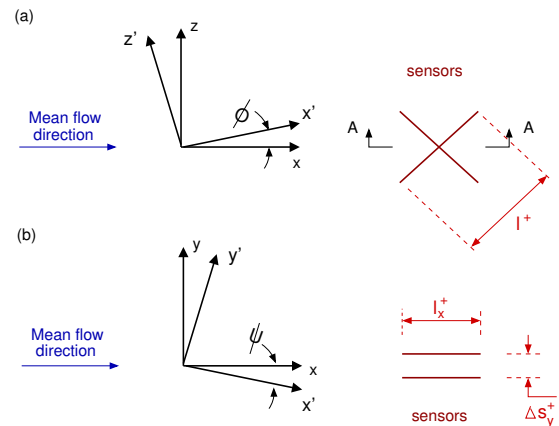


Figure 1. A schematic representation of the misalignment between the wind-tunnel coordinate system (x - y - z) and the coordinate system for the 2-D jet calibrator (x' - y' - z') for an X-probe oriented to measure the u and w velocities. The angles in (a) ϕ and (b) ψ correspond to the in-plane and out-of-plane misalignment with reference to the sensor plane, respectively.

angular offsets only within $\phi, \psi \approx \pm 0.5^\circ$, which is the accuracy level obtained when the jet calibrator is aligned with the probe using some references (eg. laser sheets).

The problem becomes serious when there are no references available to aid the alignment procedure. Such a situation may be encountered when the multi-wire probes are not calibrated *in situ*, i.e. probes need to be unmounted from the traverse in tunnel to calibrate at a different location. *In situ* calibration of a multi-wire probe, which is to be used for measurement in an internal flow geometry (eg. channel, pipe flow), is also challenging given that the jet calibrator cannot be taken inside the working section due to physical constraints (in a majority of cases). The angular offset (ϕ, ψ), which signifies the degree of misalignment in the 2-D calibration, can be greater than 2° degrees (shown later) in such cases and hence cannot be accounted for by using the methodology implemented by Baidya *et al.* (2019a). In the present study, we encountered a similar scenario while attempting to conduct velocity profile measurements using an X-probe in a channel flow facility. Here, we attempt to

Probe	Ref.	Re_τ	Probe type	Flow type	h or δ (in m)	ν/U_τ (in μm)	θ_w (in deg)	l_x^+ , l_y^+	Δs_z^+	Symbol	Misaligned 2-D Cal only
A55P51AX1	1,000	uv	Channel	0.05	50	45	14	10	▲	✓	
A55P61AX2	1,000	uv	Channel	0.05	50	45	7	10	▼	✓	
CustomCX	1,000	uv	Channel	0.05	50	45	7	4	◆	✓	
	10,000	uv	ZPG TBL	0.32	32	45	12	7	●		

Table 1. A summary of the various physical experiments conducted. Terminology has been described in the text below and in figure 1. Synthetic experiments were conducted corresponding to the inner-scaled measuring volume for each case mentioned. Statistics from these synthetic experiments are plotted with the same symbol and a lighter color shade as for the corresponding physical experiments.

highlight the effect of such a calibration misalignment on the velocity statistics and spectra, followed by proposal of a technique to correct the erroneous velocity statistics using synthetic experiments as a reference.

EXPERIMENTAL SET-UP

Physical experiments

Physical experiments were conducted in the channel flow facility and the high Reynolds number boundary layer wind tunnel (HRNBLWT) housed in the University of Melbourne. Table 1 lists the details of the various X-probes used in the physical experiments, which differ in terms of their viscous-scaled measuring volumes. Here, the superscript ‘+’ denotes normalization in viscous units and capitalization indicates time-averaged quantities. 2-D calibration of these X-probes was performed *in situ* with an articulating compressed-air driven jet facility. The facility comprises of a jet mounted on a frame allowing rotation in both the pitch and yaw directions (jet rotation defined by θ). For an accurately aligned jet (i.e. $\phi, \psi \approx 0^\circ$; figure 1), the jet flow direction is oriented along the streamwise direction of the tunnel for a jet angle, $\theta = 0^\circ$. A sweep of the jet angles (θ) is carried out for multiple jet velocities (U_{jet}) to record the corresponding voltages from the wire 1 and wire 2 (E_1 and E_2) and obtain a one-to-one mapping between the voltage-velocity pairs following: $E_1 = a(U_{jet}, \theta)$ and $E_2 = b(U_{jet}, \theta)$. Figure 2(a) shows the voltage pairs acquired during a 2-D calibration as an example. Apart from the 2-D calibration, another calibration (henceforth referred as 1-D calibration) is performed by traversing the X-probe to the free-stream (or centreline in case of the channel) and recording voltages corresponding to various free-stream speeds in turn estimated through a Pitot-static tube. This calibration is similar to the conventional calibration for a single-wire hotwire sensor (Talluru *et al.*, 2014) and is used as a reference to check for misalignment between the tunnel coordinate system and the coordinate system for the jet calibrator (Baidya *et al.*, 2019a). For an accurately aligned jet calibrator, the voltage pairs corresponding to $\theta = 0^\circ$ during the 2-D calibration, for various U_{jet} , should align with the voltage pairs recorded during 1-D calibration.

In case of measurements in the boundary layer tunnel, the entire jet calibrator set-up could be arranged inside the test section. It allowed for an accurate alignment of the jet coordinate system with the tunnel coordinate system through the use of laser sheets. Hence, an ‘accurate’ 2-D calibration (i.e. $\phi, \psi \approx 0^\circ$) of the X-probe could be achieved during the boundary layer measurement. Another calibration was carried out for the same X-probe, immediately after the *accurate* 2-D calibration, where the jet was purposely *misaligned* by a random angle ($\phi, \psi \neq 0^\circ$) with respect to the measurement coordinate system.

During channel flow measurements, given the limited cross-section of the working section ($1,170 \times 100 \text{ mm}^2$), the X-probe was traversed outside of this section. The jet facility was positioned on the top surface of the working section. However, unlike the case of the boundary layer tunnel, there were no reliable reference planes at the channel top for accurately aligning the jet using laser sheets. Hence, the alignment of the jet with respect to the channel coordinate system was always carried out through visual inspection, a method which is prone to lead to misalignment ($\phi, \psi \neq 0^\circ$). Accordingly, as marked in table 1, all the 2-D calibrations in case of the channel flow measurements were misaligned.

Synthetic experiments

Synthetic probe experiments were conducted through the use of channel DNS data of del Alamo *et al.* (2004) at $Re_\tau = 934$. The synthetic experiments (Philip *et al.*, 2013; Baidya, 2016) are based on the argument that the spatial attenuation corresponding to sensor measuring volume scales with viscous units (i.e. independent of Re_τ). Here, we compare the spatially filtered statistics from the synthetic experiments with those from physical experiments and the differences between the two are assigned to calibration misalignment. To this end, spatially filtered velocity fields are computed for each X-probe measuring volume mentioned in table 1, from which the statistics and spectra are obtained at the same wall-normal locations as the corresponding physical experiment (limited up to $z^+ \leq 934$).

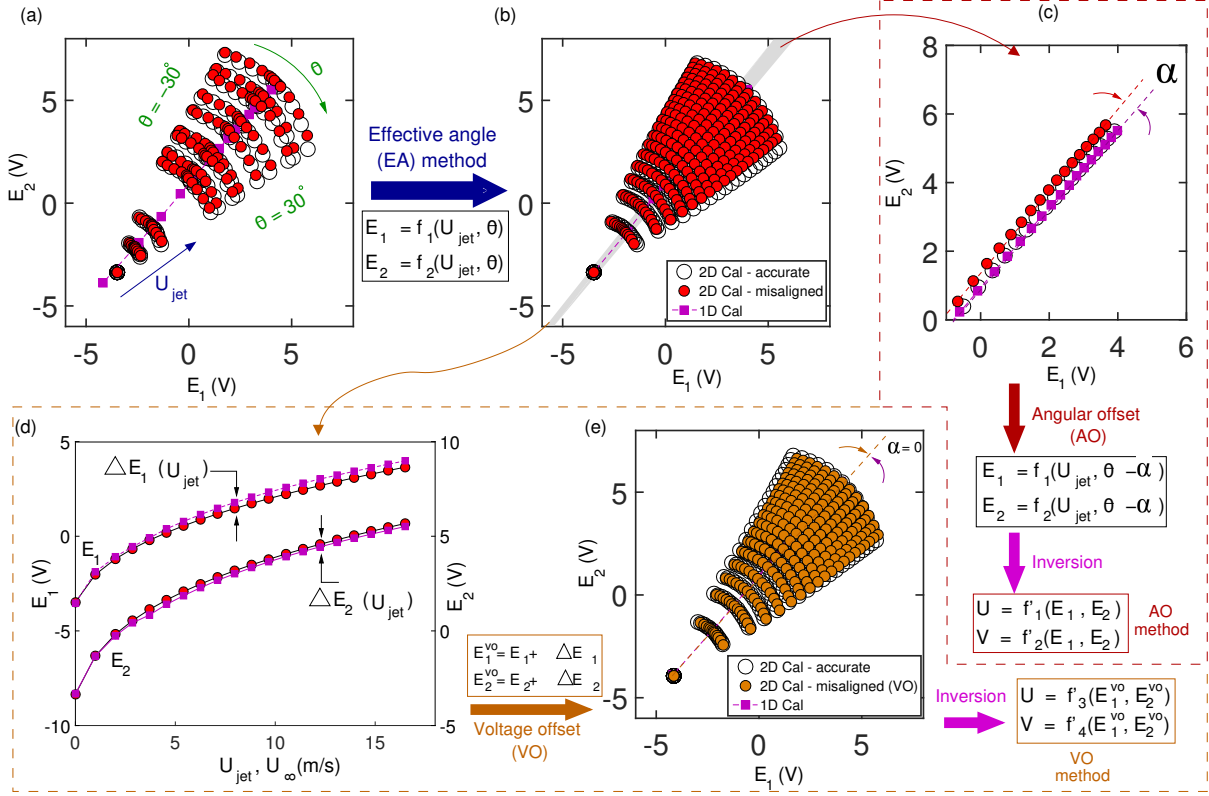


Figure 2. Procedure to account for misalignment while processing 2-D calibration of an X-probe, explained by using an ‘accurate’ 2-D calibration as a reference: (a) Voltage pairs obtained by varying the U_{jet} and θ for an *accurate* and misaligned 2-D calibration along with the voltages obtained from the pre 1-D calibration in the tunnel. (b) Voltages in (a) interpolated onto a linearly distributed set of U_{jet} and θ based on effective angle method. (c) Comparison of 2-D calibration voltage pairs corresponding to $\theta = 0^\circ$ (highlighted by gray background in (b)) with 1-D calibration to obtain the angular offset α . (d) The same voltage pairs as in (c), but compared individually for the two sensors to obtain the voltage offset $\Delta E_1(U_{jet})$ and $\Delta E_2(U_{jet})$. (e) Comparison between voltage pairs from the *accurate* calibration and the misaligned calibration, with the latter shifted after application of the voltage offset estimated in (d).

2-D CALIBRATION MISALIGNMENT

In this section, we discuss possible ways to identify and account for calibration misalignment before generating the calibration surfaces for processing the velocity time series. For this, we consider the two 2-D calibrations - *accurate* and misaligned, conducted for a CX probe before the high Re_τ boundary layer (TBL) measurement in HRNBLWT with the same probe. Both these calibrations are used to process this boundary layer data set, to compute the velocity statistics and spectra, allowing us to understand the effect of misalignment on these statistics.

Identification and subsequent processing

Figure 2 gives a flowchart-type description of identifying a misaligned calibration followed by two possible ways of accounting for it while processing. Figure 2(a) shows the mean voltages acquired during the *accurate* and misaligned 2-D calibration of the CX probe for various U_{jet} and θ . Also plotted are the mean voltages acquired during the pre 1-D calibration. To make a meaningful comparison, the voltage pairs acquired during both the 2-D calibrations are fitted to smooth functions of jet velocity and angles based on the effective angle method (Bradshaw,

2013), which are then solved for a linearly distributed set of U_{jet} and θ . The 1-D calibration is also interpolated over the same range of U_{jet} and the three calibrations are re-plotted in figure 2(b) for comparison. The difference between the misaligned and the *accurate* 2-D calibration is apparent.

To estimate the angular offset (α) between the coordinate system for the tunnel and the 2-D calibration, we compare the voltage pairs recorded at $\theta = 0^\circ$ at various U_{jet} (henceforth referred as θ_o points) during both the 2-D calibrations with the 1-D calibration voltages in figure 2(c). The voltage pairs corresponding to θ_o from the misaligned 2-D calibration are way off from the 1-D calibration, highlighting the misalignment which is denoted by α in figure 2(c). $\alpha \approx 2.5^\circ$ for the case shown in figure 2(c). One of the methods of processing a misaligned calibration is by accounting for the estimated angle α in the calibration map as follows: $E_1 = f_1(U_{jet}, \theta - \alpha)$ and $E_2 = f_2(U_{jet}, \theta - \alpha)$, i.e. subtracting α across the entire set of θ considered. The calibration surfaces f'_1 and f'_2 for U and V respectively, are obtained on inverting the calibration map with the jet angles offset with α . This method is henceforth referred as angular offset (AO) method and is the same as utilised by Baidya *et al.* (2019a) to account for small misalignment.

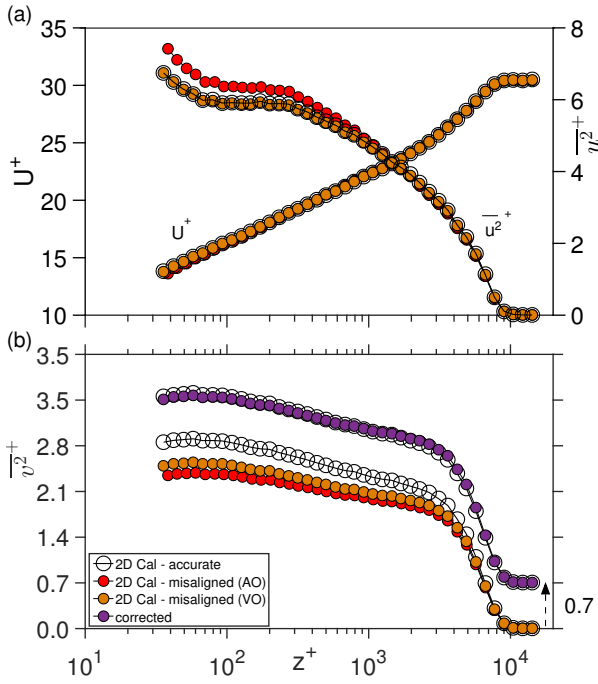


Figure 3. Inner-scaled profiles of (a) mean streamwise velocity and streamwise turbulence intensity and (b) spanwise turbulence intensity obtained on processing the high Re_τ boundary layer data set using the *accurate* and misaligned 2-D calibrations. In (b), the corrected turbulence intensity is plotted with a vertical shift and compared with $\overline{v^2}^+$ obtained from the *accurate* 2-D calibration.

Given that $\alpha \approx 2.5^\circ$ for the present experiment, which is beyond the scope for correction using the *AO* method, we propose another method to account for misalignment wherein we force α to 0° by offsetting the calibration voltages (instead of the jet angles) before inverting to find the U, V surfaces. We do this by forcing the 2-D calibration voltage pairs corresponding to θ_o , to be equivalent to those recorded during the 1-D calibration. Figure 2(d) plots these voltages from the two sensors (same as shown in figure 2(c)) against U_{jet} and U_∞ for the case of the misaligned 2-D calibration and the 1-D calibration, respectively. Based on the comparison, a unique voltage offset is estimated for both the sensors (as a function of U_{jet}) for the voltages to overlap. Next, the voltage offsets for both the hotwire sensors, $\Delta E_1(U_{jet})$ and $\Delta E_2(U_{jet})$, are applied across the entire calibration map. Figure 2(e) shows the resulting ‘offset’ 2-D calibration with α forced to 0. The calibration surfaces for U (f'_3) and V (f'_4) are obtained by inverting this 2-D calibration map. This method of accounting for misalignment is henceforth referred as voltage offset (*VO*) method. We shall compare the performance of the two methods in the forthcoming discussion.

Effect on velocity statistics and spectra

We now process the boundary layer dataset using the two different sets of calibration surfaces obtained from the misaligned 2-D calibration via the *AO* and *VO* methods, along with the calibration surfaces

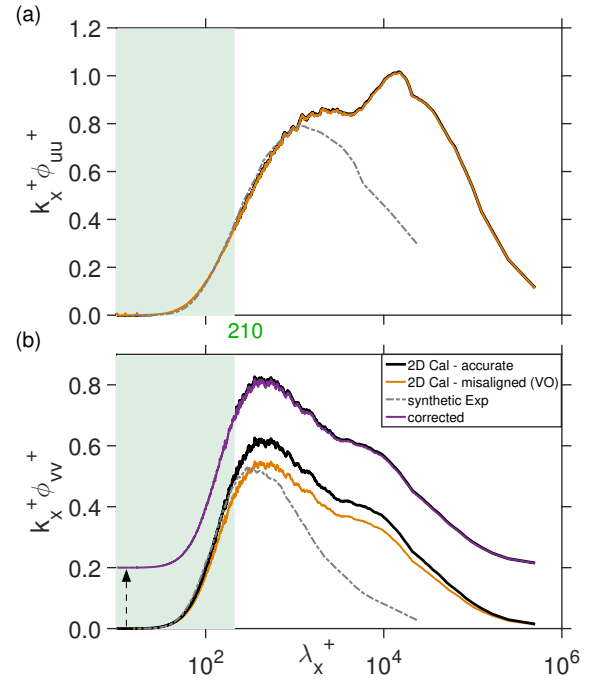


Figure 4. Inner-scaled 1-D premultiplied streamwise energy spectra of the (a) streamwise and (b) spanwise velocity obtained on processing the high Re_τ boundary layer data set using the *accurate* and misaligned 2-D calibrations and from the corresponding synthetic experiment. In (b), the corrected spectra of the spanwise velocity is plotted with a vertical shift and compared with spectra obtained from the *accurate* 2-D calibration.

obtained from the *accurate* 2-D calibration. Figure 3 shows the inner-scaled mean streamwise velocity (U^+) along with streamwise ($\overline{u^2}^+$) and spanwise ($\overline{v^2}^+$) turbulence intensity processed from the aforementioned calibration surfaces.

Considering the statistics obtained through *AO* method first, $\overline{u^2}^+$ is seen to be deviating from the reference values as we go close to the wall. An appreciable difference can also be noted in the mean streamwise velocity profile for $z^+ < 100$. On the other hand, if we consider the streamwise statistics processed using *VO* method, both U^+ and $\overline{u^2}^+$ are similar to the reference statistics. Coming to the spanwise turbulence intensity (figure 3(b)), $\overline{v^2}^+$ estimated from both the misaligned 2-D calibrations (using *AO* and *VO* methods) deviate from the reference values as the wall is approached. Relatively, the error in $\overline{v^2}^+$ estimated from *AO* method is larger than that estimated from *VO* method. Since the later performs better than the former, by yielding reasonably accurate streamwise statistics, only the *VO* method of processing the misaligned calibration is considered henceforth. The fact that $\overline{v^2}^+$ estimated from this method deviates from the reference values may be attributed to the application of a voltage offset independent of θ ($\Delta E_1(U_{jet})$, $\Delta E_2(U_{jet})$), which incorrectly assumes a linear response of the hotwire sensor to flow angles (Hinze, 1975; Bradshaw, 2013).

To further investigate the effect of a misaligned 2-D calibration, we compare the inner-scaled premultiplied 1-D streamwise energy spectra of both the streamwise ($k_x^+ \phi_{uu}^+$) as well as spanwise ($k_x^+ \phi_{vv}^+$) velocity components at $z^+ = 100$ in figure 4. Also plotted is the premultiplied spectra obtained from the synthetic experiment corresponding to the X-probe used in the physical experiment. This is done with the intention to invoke the following argument of Hutchins *et al.* (2009): the viscous-scaled small-scale turbulence energy is invariant with Re_τ and solely depends on the inner-normalized spatial resolution of the sensor. Although Hutchins *et al.* (2009) demonstrated this only for the u velocity component, Baidya (2016) has shown that the same argument also holds for the v and w components. It was found, based on careful observation, that energy contained in the scales smaller than $\lambda_x^+ \approx 210$ should be consistent with the premise for all three velocity components. Thus, ideally, one should see an overlap of $k_x^+ \phi_{ii}^+(\lambda_x^+; z^+)$ at various Re_τ for $\lambda_x^+ < 210$, where $i = u, v$ or w . This range has subsequently been highlighted in the background in figure 4 for reference. Here, $\lambda_x = 2\pi/k_x$ where k_x is the streamwise wavenumber and is obtained from the temporal frequency by invoking the Taylor's hypothesis which assumes the convection velocity (U_c) for all scales is equal to $U(z^+)$.

The spectra of the streamwise velocity, processed via the misaligned calibration ($(k_x^+ \phi_{uu}^+)_{Exp}$), compares well with the reference spectra from the accurate 2-D calibration (figure 4(a)). It also compares well with the spectra obtained from the synthetic experiments ($(k_x^+ \phi_{uu}^+)_{sDNS}$), in the small scale range. However, in case of the spanwise velocity spectra, the energy distribution obtained by processing from a misaligned calibration seems to be attenuated across the entire range of scales (λ_x^+) when compared to the reference spectra from the 'accurate' calibration (figure 4(b)). Interestingly, the shape/form of the spectra obtained from the misaligned calibration is similar to that of the reference spectra and the former appears to be an attenuated version of the latter. This is confirmed on comparing the erroneous spectra with that obtained from the synthetic experiment where a clear attenuation of the energy can be seen in the small scale range. A similar trend is noted on comparing the spectra at all z^+ (not shown here). Since the turbulence intensity is the integral of the 1-D spectra over all the scales, the $\overline{v^2}^+$ profile from the misaligned calibration also appears to be an attenuated version of the reference profile (figure 3(b)). This mismatch, in the small scale range, is thus considered to be an artefact of the misaligned calibration. Following the aforementioned premise, we propose a methodology to force a collapse of $(k_x^+ \phi_{vv}^+)_{Exp}$ onto the corresponding $(k_x^+ \phi_{vv}^+)_{sDNS}$, for $\lambda_x^+ < 210$, by computing a correction ratio.

CORRECTION SCHEME

The idea here is to correct the $(k_x^+ \phi_{vv}^+)_{Exp}$ ($0 < \lambda_x^+ < \infty; z^+$) obtained from the misaligned 2-D calibration using $(k_x^+ \phi_{vv}^+)_{sDNS}$ ($\lambda_x^+ < 210; z^+$) obtained from the corresponding synthetic experiment as a ref-

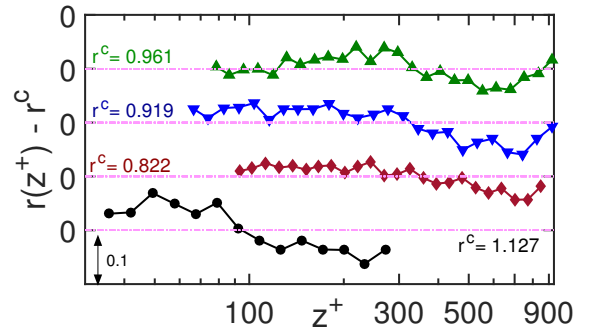


Figure 5. Deviation of r from the correction ratio r^c across the velocity profile measurement locations (z^+), computed for the physical experiments for which a misaligned calibration was obtained. Symbols represent physical experiments with various X-probes as mentioned in table 1. For the case of high Re_τ experimental data (\circ), r^c is calculated by considering $r(z^+)$ only up to $z^+ \approx 300$ and hence deviations for only those points have been shown.

erence. To this end, we propose to compute a ratio (r) for every z^+ as follows:

$$r(z^+) = \frac{\overline{\left(\frac{(k_x^+ \phi_{vv}^+(\lambda_x^+; z^+))_{sDNS}}{(k_x^+ \phi_{vv}^+(\lambda_x^+; z^+))_{Exp}} \right)}}{\quad} \quad (1)$$

for $190 < \lambda_x^+ < 210$.

Following this definition, the ratio r is computed individually at each z^+ up to $z^+ = 934$, which is limited by the DNS dataset. We take the mean value, $r^c = \overline{r(z^+)}$ to be considered as the unique correction ratio for $(k_x^+ \phi_{vv}^+)_{Exp}$ ($0 < \lambda_x^+ < \infty; 0 < z^+ < \delta^+$), i.e. to correct for the entire velocity profile. Figure 5 depicts the variation of $(r(z^+) - r^c)$ with z^+ for all the velocity profile measurements listed in table 1. r^c appears to be a reasonably good representative value as a unique correction ratio since r doesn't vary significantly with z^+ .

The correction ratio, r^c is used as a *gain* to amplify or attenuate the premultiplied 1-D spectra as follows: $(k_x^+ \phi_{vv}^+)^c_{Exp} = r^c (k_x^+ \phi_{vv}^+)_{Exp}$, where $(k_x^+ \phi_{vv}^+)^c_{Exp}$ is the corrected spectra. Figure 4(b) shows the corrected version of the premultiplied 1-D spectra for the spanwise velocity component. It can be observed that although r^c was estimated purely based on the spectra in the range $190 < \lambda_x^+ < 210$, the corrected experimental spectra shows a reasonable overlap with the reference ('accurate') spectra across all λ_x^+ . Similar observation is noted for the spectra at all z^+ , suggesting that a unique correction ratio for the entire velocity profile (r^c) performs reasonably well. Consideration of r^c for correcting statistics at all wall normal locations is advantageous for the following two reasons: (i) the corrected statistics ($\overline{v^2}/w^2$) would vary smoothly with distance from the wall, and (ii) the same r^c could be applied to $z^+ > 934$, i.e. while correcting for high Re_τ datasets.

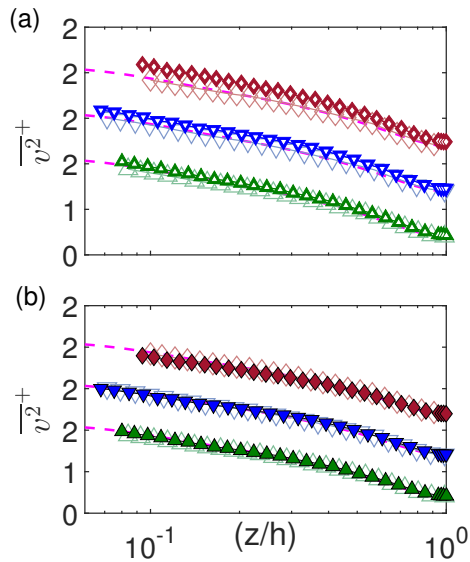


Figure 6. (a) Uncorrected (dark, partially-filled) and (b) corrected (dark, fully-filled) spanwise stresses for the $Re_\tau \approx 1,000$ channel flow experiments. Symbols represent experiments with various X-probes as mentioned in table 1. Empty symbols in light shading represent statistics from the corresponding synthetic experiments. (- -) represents the unfiltered statistics from the channel DNS at $Re_\tau = 934$.

Comparing uncorrected and corrected statistics

Figure 6 depicts the uncorrected and corrected statistics from the velocity profile measurements using various X-probes in the channel flow at $Re_\tau \approx 1000$. Corrected $\overline{v^2}^+$ profile is obtained by simply integrating the corrected 1-D spectra at each z^+ . Also plotted, are the statistics from the corresponding synthetic experiments on the channel DNS dataset. Corrected statistics for the high Re_τ TBL measurements are shown in figure 3(b).

As discussed previously, profiles of the uncorrected $\overline{v^2}^+$ from the physical experiments indeed appear to be an amplified or attenuated version of those from the corresponding synthetic experiments (figure 6(a)). On correction using r^c , the two profiles compare reasonably well for all the experiments (figure 6(b)). This supports the idea of using a unique correction ratio, r^c for the entire velocity profile.

SUMMARY

The present study experimentally investigated the effect of misalignment between the calibration and tunnel coordinate system for an X-probe calibration. The emphasis was on a scenario where the calibration is severely misaligned ($\alpha > 2^\circ$) due to the absence of reference planes required to accurately orient the calibration jet with the probe. The turbulent stress profiles of the lateral velocity components, when processed from the misaligned calibration, appeared to be either amplified or attenuated relative to the expected profiles. The consistent nature of deviation of the erroneous statistics inspired the proposal of a correction scheme to rectify the errors. The expected

velocity statistics and spectral distribution was obtained via conducting synthetic experiments on well-resolved DNS fields. The scheme thus depends on the availability of these fields since the spectral energy distribution is a function of the viscous-scaled spatial resolution of the sensor used, which would be unique for each experiment. The correction scheme shows promising results when applied to wall turbulence measurements conducted across a decade of Re_τ and using X-probes of varying spatial resolution.

ACKNOWLEDGEMENT

The authors would like to thank Dr. Rio Baidya for helpful discussions and sharing his code for the synthetic experiments on the DNS data set. The authors also gratefully acknowledge the financial support from the Australian Research Council.

REFERENCES

- del Alamo, J. C., Jiménez, J., Zandonade, P. & Moser, R. D. 2004 Scaling of the energy spectra of turbulent channels. *Journal of Fluid Mechanics* **500**, 135–144.
- Baidya, R. 2016 Multi-component velocity measurements in turbulent boundary layers. PhD thesis, University of Melbourne, Department of Mechanical and Manufacturing Engineering.
- Baidya, R., Philip, J, Hutchins, N, Monty, JP & Marusic, I 2019a Sensitivity of turbulent stresses in boundary layers to cross-wire probe uncertainties in the geometry and calibration procedure. *Measurement Science and Technology, (in press)*.
- Baidya, R., Philip, J., Hutchins, N., Monty, J.P. & Marusic, I. 2019b Spatial averaging effects on the streamwise and wall-normal velocity measurements in a wall-bounded turbulence using a cross-wire probe. *Measurement Science and Technology, (submitted)*.
- Bradshaw, P. 2013 *An introduction to turbulence and its measurement: thermodynamics and fluid mechanics series*. Elsevier.
- Hinze, J. 1975 *Turbulence*. McGraw-Hill, New York.
- Hutchins, N., Nickels, T. B., Marusic, I. & Chong, M. S. 2009 Hot-wire spatial resolution issues in wall-bounded turbulence. *Journal of Fluid Mechanics* **635**, 103–136.
- Jørgensen, F.E. 1996 The computer-controlled constant-temperature anemometer. aspects of setup, probe calibration, data acquisition and data conversion. *Measurement Science and Technology* **7** (10), 1378.
- Philip, J., Baidya, R., Hutchins, N., Monty, J. P. & Marusic, I. 2013 Spatial averaging of streamwise and spanwise velocity measurements in wall-bounded turbulence using v- and x-probes. *Measurement Science and Technology* **24** (11), 115302.
- Talluru, K.M., Kulandaivelu, V., Hutchins, N. & Marusic, I. 2014 A calibration technique to correct sensor drift issues in hot-wire anemometry. *Measurement Science and Technology* **25** (10), 105304.
- Yavuzkurt, S. 1984 A guide to uncertainty analysis of hot-wire data. *ASME, Transactions, Journal of Fluids Engineering* **106** (2), 181–186.